Solution Calorimetric and Stopped-Flow Kinetic Study of Ligand Substitution for the Complexes $M(CO)_3(PCy_3)_2(L)$ (M = Cr, Mo, W). Comparison of First-, Second-, and Third-Row Transition-Metal-Ligand Bonds at a Sterically Crowded Metal Center

Kai Zhang,[†] Alberto A. Gonzalez,[†] Shakti L. Mukerjee,[†] Shou-Jiau Chou,[†] Carl D. Hoff,*[,†] Kimberly A. Kubat-Martin,[‡] David Barnhart,[‡] and Gregory J. Kubas*[,‡]

Contribution from the Department of Chemistry, University of Miami, Coral Gables, Florida 33124, and Los Alamos National Laboratory, Los Alamos, New Mexico 87545. *Received March 25, 1991*

Abstract: The substitution of pyridine by trimethyl phosphite in the complexes $M(CO)_3(PCy_3)_2(py)$ (M = Cr, Mo) has been studied by stopped-flow kinetics. Direct reactions of the proposed intermediate complexes $M(CO)_3(PCy_3)_2$ (M = Cr, Mo) have also been studied. The crystal structure of $Cr(CO)_3(PCy_3)_2$ has been determined and shows an an agostic M···H-C interaction. Cell parameters: a = 10.127 (2) Å, b = 12.524 (3) Å, c = 15.329 (3) Å, β = 90.93 (3)°, γ = 103.28 (3)°, space group $P\bar{1}$, Z = 2. These results are combined with calorimetric measurements, and with earlier data on the isostructural W complex, to give a complete picture of ligand substitution in these sterically crowded complexes. The relative rates of dissociation of the M-py bond are in the order Cr > Mo > W in the approximate ratio 4800/300/1. The relative rates of reaction of the formally coordinatively unsaturated complexes $M(CO)_3(PCy_3)_2$ with trimethyl phosphite are in the order Mo > W > Cr in the approximate ratio 80/36/1. Due to these changes in relative magnitude for the rate constants, the chromium complex does not obey simple steady-state kinetics. Solution calorimetric measurements show that the enthalpies of binding of pyridine and trimethyl phosphite are as follows: W, -19 and -26 kcal/mol; Mo, -17 and -24 kcal/mol; Cr, -16 and -11 kcal/mol. Enthalpies of activation for dissociation of pyridine: W, -22.6 kcal/mol; Mo, -21.9 kcal/mol; Cr, -15.1 kcal/mol. The activation energy for addition of py to $M(CO)_3(PCy_3)_2$ is about 4 kcal/mol for all three metals and probably involves concerted attack at the agostic bond.

Introduction

The role of steric factors in organometallic chemistry has been widely investigated,[1] but there are few quantitative studies of ligand binding in severely crowded molecular systems. The complexes $M(CO)_3(PCy_3)_2$ (M = Cr, Mo, W)[2,3] present the opportunity to investigate kinetic and thermodynamic aspects of ligand binding in a well-defined but sterically demanding environment. The parent W complex exhibits size-selective binding of ligands.[2] We have reported earlier[4] a solution calorimetric study of ligand binding to the tungsten complex as shown in eq 1.

$$W(CO)_3(PCy_3)_2 + L \rightarrow W(CO)_3(PCy_3)_2(L) \qquad (1)$$

$$L = H_2, N_2, CH_3CN, py, PPh_2Me, P(OMe)_3, CO$$

The stable but highly air-sensitive complexes $M(CO)_3(PCy_3)_2$ resemble unstable intermediates which are normally studied under flash photolysis conditions.[5] For example, it is now well established that "naked" $M(CO)_5$ in alkane solution has an extremely short lifetime and is rapidly solvated:[6,7]

$$Cr(CO)_6 \xrightarrow[-CO]{h\nu} Cr(CO)_5 \xrightarrow{C_6H_{12}} Cr(CO)_5(C_6H_{12}) \xrightarrow[-C_6H_{12}]{L} Cr(CO)_5(L) \qquad (2)$$

The reactions normally observed for "$Cr(CO)_5$" are actually those of the agostic complex $Cr(CO)_5(C_6H_{12})$, which has a three-center $Cr\cdots H-C_6H_{11}$ bond. The crystal structure of $W(CO)_3(PCy_3)_2$ indicates that this formally "coordinatively unsaturated" complex also has an "agostic" bond between tungsten and one of the cyclohexyl groups on the phosphine ligand.[2] As we have shown in previous kinetic studies,[8] the rates of reaction of the complex $W(CO)_3(PCy_3)_2$ are about 1 order of magnitude slower than those of the corresponding reactions of $M(CO)_5$(alkane) complexes. In this paper, we report solution calorimetric and stopped-flow kinetic data on the analogous Cr and Mo complexes as well as the structure of the Cr complex. This work gives a good picture of the role of metal size in ligand substitution reactions.

Experimental Section

Manipulations involving organometallic complexes were performed under an argon atmosphere using either standard Schlenk tube techniques or a Vacuum Atmospheres glovebox. Toluene was purified by distillation from sodium benzophenone ketyl. Pyridine was purified by extended reflux over BaO followed by distillation and collection of a middle cut of the distillation. $Mo(CO)_3(PCy_3)_2$ and $Cr(CO)_3(PCy_3)_2$ were prepared by literature procedures,[2,3] and only analytically pure samples were used for all physical measurements. Infrared spectra were recorded on a Perkin-Elmer 1850 FTIR spectrometer. Kinetic measurements were made on a Hi-Tech SF-51 stopped-flow apparatus equipped with an SU-40 spectrophotometer unit. Calorimetric measurements were made on a Setaram C-80 Calvet calorimeter. Typical procedures for obtaining calorimetric and kinetic data are described below.

Measurement of the Heat of Reaction of $Mo(CO)_3(PCy_3)_2$ with Pyridine. A solution of 0.1029 g of $Mo(CO)_3(PCy_3)_2$ in 10 mL of freshly distilled toluene was prepared in the glovebox. The solution was filtered and loaded into a cell of the Calvet calorimeter equipped with a rubber septum. A separate sample of solution was withdrawn and its FTIR spectrum recorded. A separate solution of pyridine (1.26 M) in toluene was prepared. The syringe and cell were loaded into the calorimeter and allowed to equilibrate. After about 2 h, 20.0 μL of solution was added. The enthalpy of the reaction, calculated by using pyridine as the limiting

[†] University of Miami.
[‡] Los Alamos National Laboratory.

(1) (a) Darensbourg, D. J. *Adv. Organomet. Chem.* **1982**, *21*, 113 and references therein. (b) Atwood, J. D. *Inorganic and Organometallic Reaction Mechanisms*; Brooks/Cole Publishing: Monterey, CA, 1985.
(2) (a) Wasserman, H. J.; Kubas, G. J.; Ryan, R. R. *J. Am. Chem. Soc.* **1986**, *108*, 2294. (b) Kubas, G. J. *Organomet. Synth.* **1986**, *3*, 254. (c) Kubas, G. J. *Acc. Chem. Res.* **1988**, *21*, 120.
(3) Gonzalez, A. A.; Hoff, C. D. *J. Am. Chem. Soc.* **1988**, *110*, 4419.
(4) Gonzalez, A. A.; Zhang, K.; Nolan, S. P.; de la Vega, R. L.; Mukerjee, S. L.; Hoff, C. D.; Kubas, G. J. *Organometallics* **1988**, *7*, 2429.
(5) (a) Poliakoff, M.; Weitz, E. *Adv. Organomet. Chem.* **1986**, *25*, 277. (b) Weitz, E. *J. Phys. Chem.* **1987**, *91*, 3945.
(6) (a) Wang, L.; Zhu, X.; Spears, K. G. *J. Am. Chem. Soc.* **1988**, *110*, 8695. (b) Wang, L.; Zhu, X.; Spears, K. G. *J. Phys. Chem.* **1989**, *93*, 291.
(7) Xie, X.; Simon, J. D. *J. Phys. Chem.* **1989**, *93*, 4401.
(8) (a) Zhang, K.; Gonzalez, A. A.; Hoff, C. D. *J. Am. Chem. Soc.* **1989**, *111*, 3627. (b) Gonzalez, A. A.; Zhang, K.; Hoff, C. D. *Inorg. Chem.* **1989**, *28*, 4285. (c) Gonzalez, A. A.; Zhang, K.; Hoff, C. D. *Inorg. Chem.* **1989**, *28*, 4295. (d) Gonzalez, A. A.; Zhang, K.; Mukerjee, S. L.; Hoff, C. D. Unpublished results.

0002-7863/91/1513-9170$02.50/0

Table I. Structure Determination Summary

Crystal Data	
empirical formula	$C_{39}H_{66}CrO_3P_2$
color; habit	black; rhomb
cryst size, mm	0.1 × 0.2 × 0.2
cryst system	triclinic
space group	$P\bar{1}$
unit cell dimens	
a, Å	10.127 (2)
b, Å	12.524 (3)
c, Å	15.329 (3)
α, deg	91.18 (3)
β, deg	90.93 (3)
γ, deg	103.28 (3)
V, Å^3	1891.4 (7)
Z	2
fw	696.9
density (calc), Mg/m^3	1.224
abs coeff, mm^{-1}	0.411
F(000)	756
Data Collection	
diffractometer used	Enraf-Nonius CAD4
radiation (λ, Å)	Mo Kα (0.71073)
temp, °C	−70
monochromator	highly oriented graphite crystal
2θ range, deg	1.4–5.5
scan type	2θ–θ
scan speed, deg/min	variable: 1.40–5.50 in ω
scan range (ω), deg	0.80 + 0.35 tan θ plus Kα separation
bkgd measurement	stationary crystal and stationary counter at beginning and end of scan, each for 25% of total scan time
std reflns	2 measd every 120 min
index ranges	$0 \le h \le 12$, $-14 \le k \le 14$, $-18 \le l \le 18$
tot. no. of reflns collected	7036
no. of indep reflns	5826 (R_{int} = 1.98%)
no. of obsd reflns	4302 ($F > 4.0\sigma(F)$)
abs cor	empirical
Solution and Refinement	
system used	SHELXTL PLUS (VMS)
solution	Patterson function
refinement method	full-matrix least-squares
quantity minimized	$\sum w(F_o - F_c)^2$
absolute structure	*a*
extinction cor	*a*
hydrogen atoms	refined, isotropic U
weighting scheme	$w^{-1} = \sigma^2(F) + 0.0026F^2$
no. of params refined	671
final R indices (obs data)	R = 6.18%, R_w = 8.05%
R indices (all data)	R = 9.52%, R_w = 9.00%
goodness-of-fit	1.28
largest and mean Δ/σ	0.687, 0.025
data/param ratio	6.4/1
largest difference peak, e Å^{-3}	0.81
largest difference hole, e Å^{-3}	−0.86

[a] Not applicable.

reagent, was 17.1 kcal/mol. An FTIR spectrum of the solution following calorimetry confirmed the presence of $Mo(CO)_3(PCy_3)_2(py)$ and unreacted $Mo(CO)_3(PCy_3)_2$. A small amount of $Mo(CO)_4(PCy_3)_2$ was also present. Average values for the reaction enthalpies, in this case −16.9 ± 0.6 kcal/mol for five experiments, are based on three to eight separate measurements for each reported value.

Measurement of the Rate of Reaction of $Cr(CO)_3(PCy_3)_2$ with a py/$P(OMe)_3$ Mixture. A clear blue-purple solution of $Cr(CO)_3(PCy_3)_2$ (5×10^{-4} M) in toluene was prepared inside the glovebox in one Schlenk tube, and a solution 0.400 M in $P(OMe)_3$ and 0.350 M in toluene was prepared in a second Schlenk tube. Both solutions were removed from the glovebox, and the syringes in the stopped-flow apparatus were loaded via a special manifold under argon. The syringes were flushed several times with the solution and then allowed to equilibrate at the bath temperature of 25.0 °C. Two "shots" were fired without recording the spectrum to flush the system, and then data were accumulated for the run. The reaction was monitored at 545.5 nm to show decay of the pyridine complex. The buildup of the phosphite complex, followed separately at lower wavelengths, agreed with the rate data for decay of the pyridine complex. The average value for k_{obsd} of 0.145 s^{-1} is the average of eight experiments. The value determined with a different set of stock solutions agreed within an average experimental error of 10%, typical of all kinetic data reported.

Table II. Thermodynamic Data ($-\Delta H$ in kcal/mol) for Heats of Binding of Ligands in the Complexes $M(CO)_3(PCy_3)_2$ (M = Cr, Mo, W)

	ligands			
M	$P(OMe)_3$[a]	py[a]	N_2[b]	H_2[b]
Cr	16.4 ± 0.6	11.2 ± 1.6	9.3 ± 0.2	7.3 ± 0.1
Mo	24.0 ± 1.0	16.9 ± 0.6	9.0 ± 0.6	6.5 ± 0.2
W	26.5 ± 1.5	18.9 ± 0.4	13.5 ± 1.0	10.0 ± 1.0

[a] Measured in toluene solution; values in THF overlap within experimental error. [b] Measured in THF solution; data taken from ref 8.

Structural Determination of the Complex $Cr(CO)_3(PCy_3)_2$. Crystals of the complex were grown from toluene solution upon slow cooling in a freezer. Crystal, data collection, and solution and refinement parameters for the structure are given in Table I.

Results

Calorimetric Data. The heats of reaction of $Mo(CO)_3(PCy_3)_2$ with $P(OMe)_3$ and py were measured as shown in eqs 3 and 4.

$$Mo(CO)_3(PCy_3)_2 + P(OMe)_3 \rightarrow Mo(CO)_3(PCy_3)_2(P(OMe)_3) \quad (3)$$

$$\Delta H = -24.0 \pm 1.0 \text{ kcal/mol}$$

$$Mo(CO)_3(PCy_3)_2 + py \rightarrow Mo(CO)_3(PCy_3)_2(py) \quad (4)$$

$$\Delta H = -16.9 \pm 0.6 \text{ kcal/mol}$$

As a check on these data, the enthalpy of reaction 5 was also measured. The experimental value measured for reaction 5 agrees

$$Mo(CO)_3(PCy_3)_2(py) + P(OMe)_3 \rightarrow Mo(CO)_3(PCy_3)_3(P(OMe)_3) + py \quad (5)$$

$$\Delta H = -6.5 \pm 0.4 \text{ kcal/mol}$$

within experimental error with the value of −7.1 ± 1.6 kcal/mol calculated by subtracting the ΔH of eq 4 from the ΔH of eq 3.

For the chromium complex, we were able to measure the heat of reaction with $P(OMe)_3$ as shown in eq 6. Reaction with

$$Cr(CO)_3(PCy_3)_2 + P(OMe)_3 \rightarrow Cr(CO)_3(PCy_3)_2(P(OMe)_3) \quad (6)$$

$$\Delta H = -16.4 \pm 0.6 \text{ kcal/mol}$$

pyridine, as shown in eq 4 for molybdenum, could not be measured directly for chromium, since binding of pyridine is not quantitative. Attempts to measure the equilibrium constant for binding were frustrated by the fact that the complex equilibrium shown in eq 7 is slowly established. Use of kinetic data described in the next

$$Cr(CO)_3(PCy_3)_2 + py \rightleftharpoons Cr(CO)_3(PCy_3)_2(py) \underset{PCy_3}{\overset{py}{\rightleftharpoons}} Cr(CO)_3(PCy_3)(py)_2 \underset{PCy_3}{\overset{py}{\rightleftharpoons}} Cr(CO)_3(py)_3 \quad (7)$$

section allows calculation of the enthalpy of binding of pyridine to the chromium complex. The k_{-1}/k_1 (see eq 8) ratio equals K_{eq} for binding of pyridine. From a plot of ln K_{eq} (obtained using kinetic data in Table VI) versus $1/T$, we calculated $\Delta H = -11.2 \pm 1.6$ kcal/mol and $\Delta S = -28.8 \pm 5.7$ cal/(mol deg). The value for the entropy of reaction is in reasonable agreement with that expected.[9] Thermodynamic data for ligand binding to the complexes $M(CO)_3(PCy_3)_2$ are combined in Table II.

Kinetic Measurements. All kinetic data presented can be interpreted in terms of the general reaction scheme shown in eq 8.

$$M(CO)_3(PCy_3)_2(py) \underset{k_{-1}}{\overset{k_1}{\rightleftharpoons}} py + M(CO)_3(PCy_3)_2 \xrightarrow[L]{k_2} M(CO)_3(L)(PCy_3)_2 \quad (8)$$

Two types of measurements were made in this study: direct measurements of the rate of ligand addition to the complexes $M(CO)_3(PCy_3)_2$ and net rates of ligand displacement from the

(9) (a) Benson, S. W. *Thermochemical Kinetics*, 2nd ed.; Wiley: New York, 1976. (b) Benson, S. W. *The Foundations of Chemical Kinetics*; McGraw-Hill: New York, 1960.

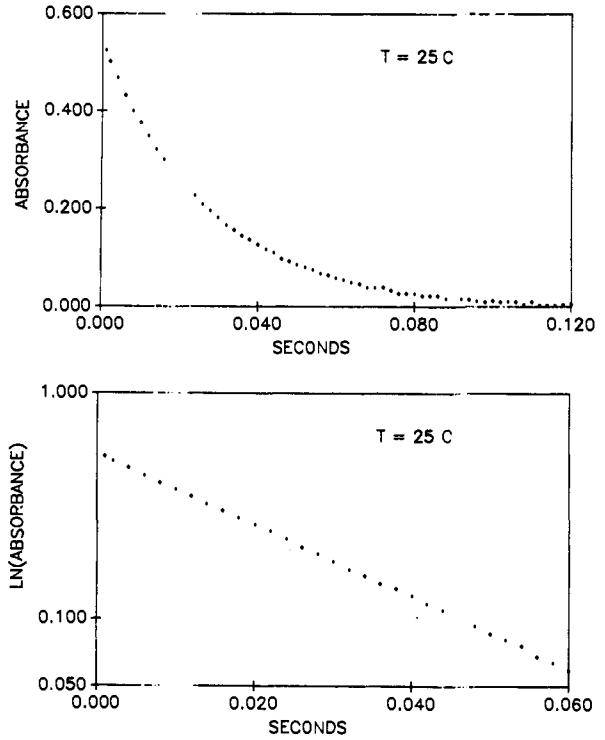

Figure 1. Experimental data on (a, top) linear and (b, bottom) logarithmic scales for reaction of $Mo(CO)_3(PCy_3)_2(py)$ with $P(OMe)_3$.

Table III. Kinetic Data for the Reaction

$Mo(CO)_3(PCy_3)_2(py) + P(OMe)_3 \rightarrow Mo(CO)_3(PCy_3)_2(P(OMe)_3)$

T, °C	$[py]/[P(OMe)_3]$	$1/k_{obsd}$, s	k_1, s^{-1}	k_{-1}/k_2
5	36.5	260.5		
	18.4	137.1		
	9.3	61.7		
	7.4	49.1		
	4.9	31.7	2.4 ± 0.4[a]	18 ± 2[b]
15	72.9	117.1		
	36.8	57.7		
	18.4	28.9		
	4.1	5.97		
	1.0	1.64		
	0.097	0.242		
	0.000	0.091	11.0 ± 1.2	17.7 ± 1.8
25	4.70	2.14		
	1.09	0.550		
	0.109	0.0769		
	0.00	0.0268	37.3 ± 4.1	16.6 ± 1.7

[a] This value calculated using an estimated value for k_{-1}/k_2 of 18. [b] Estimated value from data at 15 and 25 °C and comparison to data for W complex reported in ref 8.

complexes $M(CO)_3(PCy_3)_2(py)$. The combination of these two techniques allows determination of all the rate constants in eq 8.

Reaction of $M(CO)_3(PCy_3)_2(py)$ with $P(OMe)_3$. Molybdenum. The observed reactions are roughly 300 times faster for the molybdenum complex than for the analogous tungsten complex.[8] This required use of stopped-flow techniques for all reactions studied. Typical experimental data are shown in Figure 1. The logarithmic plot shows clearly that the reaction is first order through 4–5 half-lives.

Primary kinetic data for reaction of $Mo(CO)_3(PCy_3)_2(py)$ with $P(OMe)_3$ are listed in Table III. These data are in agreement with the mechanism proposed in eq 8. Following standard procedures, steady-state treatment of eq 8 leads to the rate law in eq 9. Under pseudo-first-order conditions, a plot of $1/k_{obsd}$ versus

$$\frac{-d[Mo_k\text{-}py]}{dt} = \frac{k_1k_2[Mo_k\text{-}py][P(OMe)_3]}{k_{-1}[py] + k_2[P(OMe)_3]} \quad (9)$$

$[py]/[P(OMe)_3]$ should have a slope of k_{-1}/k_1k_2 and an intercept of $1/k_1$ as shown in eq 10. Treatment of these data yields the calculated values of k_1 and k_{-1}/k_2 shown in Table III.

$$1/k_{obsd} = (k_{-1}/k_1k_2)[py]/[P(OMe_3)] + 1/k_1 \quad (10)$$

Table IV. Kinetic Data and Calculated Rate Constants for the Reaction

$Cr(CO)_3(PCy_3)_2 + py + P(OMe)_3 \rightarrow Cr(CO)_3(PCy_3)_2(P(OMe)_3)$

$[P(OMe)_3]$, M	$[py]/[P(OMe)_3]$	$1/k_{obsd}$, s
0.0085	3.50	0.340
0.0085	1.75	0.203
0.0085	0.875	0.145
0.017	3.50	0.300
0.017	1.75	0.169
0.017	0.875	0.107
0.051	3.89	0.292
0.051	1.94	0.154
0.051	0.972	0.0862
0.254	3.89	0.283
0.254	1.94	0.145
0.254	0.972	0.075

Chromium. Kinetic measurements in the chromium system presented several difficulties. Binding of pyridine is not quantitative, and in the absence of excess pyridine, there are appreciable amounts of the unsaturated complex present in solution. In the presence of excess pyridine, however, the equilibrium shown in eq 7 is slowly established. The solution to these problems was to alter the normal procedure used for the stopped-flow kinetics. Thus one of the syringes was loaded with $Cr(CO)_3(PCy_3)_2$ and the other was loaded with a mixture of $[py]/[P(OMe)_3]$. The net reaction which occurred was that shown in eq 11. In view

$$Cr(CO)_3(PCy_3)_2 + \{py/P(OMe)_3\} \rightarrow Cr(CO)_3(PCy_3)_2(P(OMe)_3) \quad (11)$$

of the fact that pyridine reacts some 37 times faster than phosphite, upon mixing the two solutions, a small fraction of the complex reacts directly with phosphite as shown in eq 12. The majority

$$Cr(CO)_3(PCy_3)_2 + P(OMe)_3 \xrightarrow{k_2} Cr(CO)_3(PCy_3)_2(P(OMe)_3) \quad (12)$$

of the complex reacts with pyridine first and then reacts further according to eq 8. The equilibria shown in eq 7 are established slowly on this time scale, and so reliable kinetic data could be obtained and are collected in Table III.

For the molybdenum and tungsten complexes, the rate of reaction 8 depended only on the $[py]/[P(OMe)_3]$ ratio and not on the absolute value of $[P(OMe)_3]$.[8] As shown in the data in Table IV, that was not the case for chromium. The rate of dissociation of the Cr–py bond ($t_{1/2}$ = 1 ms at 25 °C) is no longer slow compared to the other steps, and the steady-state treatment cannot be applied to the chromium complex. Full solution of this kinetic system yields two exponential decays.[9] The first one is fast and corresponds roughly to reaction 12. The slower of the two roots is what is observed in our experiments and corresponds roughly to the full mechanism in reaction 8. Rate data then obey eq 13, where $k_{-1'} = k_{-1'}[py]$ and $k_{2'} = k_2[P(OMe)_3]$:

$$k_{obsd} = \frac{k_1 + k_{-1'} + k_{2'} - [(k_1 + k_{-1'} + k_2)^2 - 4k_1k_{2'}]^{1/2}}{2} \quad (13)$$

This equation can be rearranged as follows:

$$\frac{1}{k_{obsd}} = \frac{k_1 + k_{-1'} + k_{2'} + [(k_1 + k_{-1'} + k_{2'})^2 - 4k_1k_{2'}]^{1/2}}{2k_1k_{2'}} \quad (14)$$

In the event that $4k_1k_{2'}$ is much smaller than $(k_1 + k_{-1'} + k_{2'})^2$ (which is nearly the case here), this reduces to

$$1/k_{obsd} = 1/k_1 + 1/k_2[P(OMe)_3] + \{k_{-1}/k_1k_2\}[py]/[P(OMe)_3] \quad (15)$$

For a fixed $[P(OMe)_3]$, plots of $1/k_{obsd}$ versus $[py]/[P(OMe)_3]$ should yield straight lines with slope k_{-1}/k_1k_2 and intercepts of

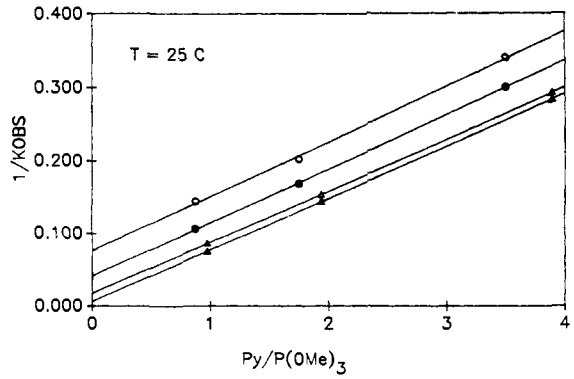

Figure 2. Plots of $1/k_{obsd}$ versus $[py]/[P(OMe)_3]$ for reaction of $Cr(CO)_3(PCy_3)_2$ with $\{py/P(OMe)_3\}$ at different absolute $[P(OMe)_3]$ (○ = 0.0085 M, ● = 0.017 M, △ = 0.051 M, ▲ = 0.254 M).

Table V. Kinetic Data[a] for the Reaction

$$M(CO)_3(PCy_3)_2 + PR_3 \rightarrow M(CO)_3(PCy_3)_2(PR_3)$$

M	L	T, °C	k_2, M^{-1} s^{-1}
Cr	$P(OMe)_3$	5	8.23×10^2
Cr	$P(OMe)_3$	15	1.16×10^3
Cr	$P(OMe)_3$	25	1.52×10^3
Mo	$P(OMe)_3$	25	1.20×10^5
Mo	PPh_2Me	25	3.61×10^4
W	$P(OMe)_3$	15	4.0×10^4
W	$P(OMe)_3$	25	5.45×10^4
W	$P(OMe)_3$	35	6.5×10^4

[a] Data for W taken from ref 8.

$1/k_1$ and $1/k_2[P(OMe)_3]$. The principal difference between the approximate eq 15 and the steady-state treatment of eq 10 is the incorporation of the term $1/k_2[P(OMe)_3]$ in the intercept. As shown in Figure 2, a series of parallel lines is generated at each different absolute concentration of $P(OMe)_3$, in accord with eq 15. Linear least-squares analysis of the slopes of the lines in Figure 6 yields a value for k_{-1}/k_1k_2 of $(7.3 \pm 0.3) \times 10^{-2}$ s^{-1}. This value is in reasonable agreement with that calculated from the directly measured individual rate constants (discussed below and combined in Table VI), which yield a combined value of $(5.4 \pm 2.4) \times 10^{-2}$ s^{-1}.

Direct Reactions of $M(CO)_3(PCy_3)_2$ with L. Molybdenum. Reaction of $Mo(CO)_3(PCy_3)_2$ with $P(OMe)_3$ (the k_2 step in eq 8) was so fast that it was on the limit of the range that can be measured by stopped-flow kinetics. Typical experimental data are shown in Figure 3. These reactions were studied using the "keyboard" technique,[10] in which the flow is interrupted during continuous monitoring of the absorption. Second-order rate constants for this reaction, as well as that with PPh_2Me, are collected in Table V. Due to the difficulty in following these reactions, temperature studies yielding activation parameters were not undertaken.

Reaction of the molybdenum complex with pyridine was too fast to measure directly using stopped-flow equipment. The value of k_{-1} can be calculated to be 2.0×10^6 M^{-1} s^{-1} from the k_{-1}/k_2 ratio of 17 and the value of $k_2 = 1.20 \times 10^5$ M^{-1} s^{-1}.

Chromium. Reaction of $Cr(CO)_3(PCy_3)_2$ with $P(OMe)_3$ was some 2 orders of magnitude slower than the reaction of the corresponding molybdenum complex. The reaction proceeds quantitatively to product, and experimental data as a function of temperature are collected in Table V. Also included in Table V are data for reaction of the tungsten complex with $P(OMe)_3$.[8b]

Due to the slower nature of ligand addition to the chromium complex, we attempted direct measurement of k_{-1} in this system. Unlike reaction with $P(OMe)_3$, which is essentially irreversible, the k_{-1} step must be included in the kinetic treatment,[9] leading to the rate law

$$k_{obsd} = k_1 + k_{-1}[py] \quad (16)$$

(10) *Instruction Manual*; Hi-Tech Scientific: Salisbury, England.

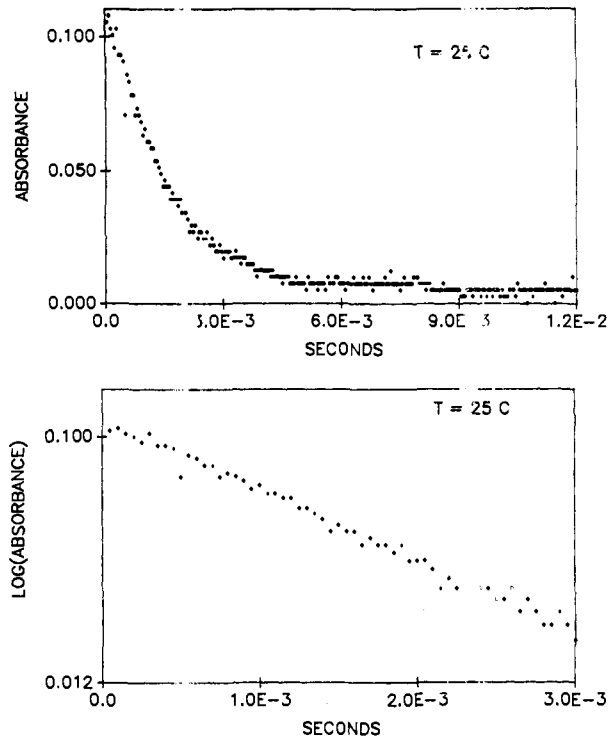

Figure 3. Experimental data on (a, top) linear and (b, bottom) logarithmic scales for reaction of $Mo(CO)_3(PCy_3)_2$ with $P(OMe)_3$.

Table VI. Kinetic Data and Calculated Rate Constants for the Reaction

$$Cr(CO)_3(PCy_3)_2 + py \underset{k_1}{\overset{k_{-1}}{\rightleftharpoons}} Cr(CO)_3(PCy_3)_2(py)$$

T, °C	[py], 10^{-2} M	k_{obsd}, s^{-1}	k_1, s^{-1}	k_{-1}, 10^4 M^{-1} s^{-1}
5	0.742	309		
	1.24	422		
	1.73	604		
	2.23	726	90 ± 30	2.86 ± 0.2
			(86)[a]	(2.89)[a]
15	0.489	432		
	0.495	445		
	0.742	499		
	0.989	630		
	1.23	717		
	1.48	800		
	1.98	951	231 ± 40	4.06 ± 0.6
			(263)[a]	(3.55)[a]
25	0.495	834		
	0.742	1038		
	0.989	1093		
	1.24	1160		
	1.48	1330	606 ± 70	4.93 ± 0.5
			(645)[a]	(4.51)[a]

[a] The values in parentheses are based on a least-squares fit of the data entered in this table as average values at each concentration. The values above them are based on complete least-squares fit of all raw data. The two values overlap within experimental error, but the upper values are preferred since they give equal weight to all experimental measurements.

Data measured for direct reaction of the chromium complex with pyridine, as a function of the pyridine concentration, are shown in Table VI. Using eq 16, a plot of k_{obsd} versus [py] should be a straight line with slope k_{-1} and intercept k_1. A least-squares fit of all data yielded the values of k_1 and k_{-1} also listed in Table VI. Rate constants at 25 °C and activation parameters are collected in Table VII.

Discussion

The goal of this work was to determine the role of the metal in ligand substitution for the sterically crowded complexes $M(CO)_3(PCy_3)_2$ (M = Cr, Mo, W). It is well-known that there

Table VII. Collected Rate Constants and Activation Parameters at 25 °C for the Reaction

$$M_k\text{-py} \underset{k_{-1}}{\overset{k_1}{\rightleftharpoons}} \text{py} + M_k + P(OMe)_3 \xrightarrow{k_2} M_k\text{-P(OMe)}_3$$

$M_k = M(CO)_3(PCy_3)_2$ (M = Cr, Mo, W)

	Cr	Mo	W
k_1, s^{-1}	606 ± 70	37 ± 4	0.125 ± 0.007
$\Delta H^{\ddagger}_{k_1}$[a]	15.1 ± 0.5	21.9 ± 1.2	22.6 ± 0.7[d]
$\Delta S^{\ddagger}_{k_1}$[b]	4.9 ± 1.6	22.6 ± 4.0	13.4 ± 2.5
$\Delta H°$[c]	11.2 ± 1.6	16.9 ± 0.6	18.9 ± 0.4
$\Delta S°$[c]	28.8 ± 5.7		
k_{-1}, M^{-1} s^{-1}	(4.9 ± 0.5) × 10^4	(2.0 ± 0.4) × 10^6	(8.6 ± 0.9) × 10^5
$\Delta H^{\ddagger}_{k_{-1}}$[a]	4.2 ± 0.9	5.0 ± 1.8	3.7 ± 1.7
k_2, M^{-1} s^{-1}	(1.5 ± 0.2) × 10^3	(1.2 ± 0.2) × 10^5	(5.5 ± 0.6) × 10^4
$\Delta H^{\ddagger}_{k_2}$[a]	4.5 ± 0.2		4.0 ± 1.3

[a] Enthalpies of activation in kcal/mol. [b] Entropies of activation in cal/(mol deg). [c] Thermodynamic data for dissociation of pyridine: $\Delta H°$ in kcal/mol, $\Delta S°$ in cal/(mol deg). [d] Data for W complex recalculated from data in ref 8. Arrhenius activation energies were reported in this paper which differ by RT from the enthalpies of activation reported here.

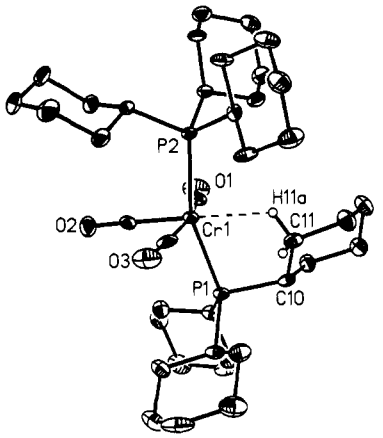

Figure 4. Ortep drawing of $Cr(CO)_3(PCy_3)_2$ (50% ellipoids), with only agostic hydrogen shown for clarity.

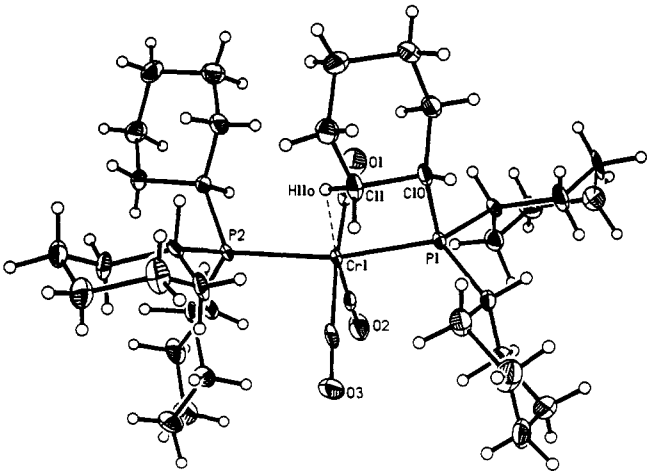

Figure 5. Ortep drawing of $Cr(CO)_3(CO)_3$, with all hydrogen atoms shown.

is a significant difference in size between first and second-row metals followed by a much smaller change in going to the third row. In some cases, the third-row congener actually has slightly smaller interatomic distances. For example, the M-C bond lengths[11] (Å) in the hexacarbonyls $M(CO)_6$ are 1.915 for Cr, 2.063 for Mo, and 2.058 for W.

(11) Bond lengths listed are an average taken from the several reported values: Kirtley, S. W. In *Comprehensive Organometallic Chemistry*; Wilkinson, G., Stone, F. G. A., Abel, E. W., Eds.; Pergamon Press: Oxford, U.K., 1982; Chapters 26.1, 27.1, and 28.1.

Table VIII. Selected Bond Distances (Å) and Angles (deg) for $(PCy_3)_2Cr(CO)_3$

	Distances		
Cr(1)-P(1)	2.342 (2)	Cr(1)-P(2)	2.386 (2)
Cr(1)-C(2)	1.803 (5)	Cr(1)-C(1)	1.864 (6)
Cr(1)-C(3)	1.866 (6)	P(1)-C(4)	1.861 (5)
P(1)-C(10)	1.860 (6)	P(1)-C(16)	1.859 (5)
P(2)-C(22)	1.853 (6)	P(2)-C(28)	1.871 (5)
P(2)-C(34)	1.889 (5)	O(2)-C(2)	1.171 (7)
O(1)-C(1)	1.167 (7)	O(3)-C(3)	1.154 (8)
	Angles		
P(1)-Cr(1)-P(2)	160.2 (1)	P(1)-Cr(1)-C(2)	101.8 (2)
P(2)-Cr(1)-C(2)	97.9 (2)	P(1)-Cr(1)-C(1)	88.6 (2)
P(2)-Cr(1)-C(1)	92.5 (2)	C(2)-Cr(1)-C(1)	82.8 (3)
P(1)-Cr(1)-C(3)	92.8 (2)	P(2)-Cr(1)-C(3)	90.9 (2)
C(2)-Cr(1)-C(3)	83.2 (2)	C(1)-Cr(1)-C(3)	165.9 (2)
Cr(1)-P(1)-C(4)	122.8 (2)	Cr(1)-P(1)-C(10)	98.8 (2)
C(4)-P(1)-C(10)	103.1 (2)	Cr(1)-P(1)-C(16)	120.0 (2)
C(4)-P(1)-C(16)	104.1 (2)	C(10)-P(1)-C(16)	105.1 (2)
Cr(1)-P(2)-C(22)	116.6 (2)	Cr(1)-P(2)-C(28)	112.5 (2)
C(22)-P(2)-C(28)	101.6 (2)	Cr(1)-P(2)-C(34)	117.3 (2)
C(22)-P(2)-C(34)	103.1 (2)	C(28)-P(2)-C(34)	103.7 (2)
Cr(1)-C(2)-O(2)	178.7 (5)	Cr(1)-C(1)-O(1)	172.2 (5)
Cr(1)-C(3)-O(3)	173.4 (5)	P(1)-C(4)-C(5)	114.9 (4)
P(1)-C(4)-C(9)	111.2 (4)	P(1)-C(10)-C(15)	115.5 (3)
P(1)-C(10)-C(11)	104.8 (4)	P(1)-C(16)-C(17)	114.3 (4)
P(1)-C(16)-C(21)	114.5 (4)	P(2)-C(22)-C(23)	114.0 (4)
P(2)-C(22)-C(27)	113.3 (4)	P(2)-C(28)-C(29)	119.7 (4)
P(2)-C(28)-C(33)	112.0 (4)	P(2)-C(34)-C(35)	115.9 (4)
P(2)-C(34)-C(39)	114.5 (4)		

Table IX. Comparison of Structural Data for $(PCy_3)_2M(CO)_3$ (M = Cr, W)

	Cr	W
M-P(1)	2.342 (1)	2.463 (1)
M-P(2)	2.386 (1)	2.494 (1)
M-C(1)	1.864 (1)	1.998 (6)
M-C(2)	1.803 (1)	1.902 (6)
M-C(3)	1.866 (1)	2.006 (6)
M···H(11a)	2.240 (1)	2.27[a]
M···C(11)	2.884 (1)	2.945 (6)
C(11)-H(11a)	0.959 (1)	0.95[a]
P(1)-M-P(2)	160.2 (1)	160.94 (4)
M-P(1)-C(10)	98.8 (1)	99.0 (2)
P(1)-C(10)-C(11)	104.8 (1)	104.7 (4)
P(1)-M···H(11a)	74.8 (1)	71.0[a]
P(2)-M···H(11a)	85.4 (1)	89.9[a]
C(1)-M···H(11a)	91.0 (1)	88.4[a]
C(2)-M···H(11a)	173.1 (1)	170.2[a]
C(3)-M···H(11a)	102.9 (1)	101.8[a]
C(11)···M···H(11a)	16.1 (1)	14.7[a]
M···H(11a)-C(11)	123.7 (1)	127.6[a]

[a] Distances and angles involving H(11a) for M = W are based on idealized coordinates for this atom with d(C-H) = 0.95 Å.

The crystal structure of the complex $Cr(CO)_3(PCy_3)_2$ is shown in Figures 4 and 5, and bond distances and angles are given in Table VIII. It is essentially isostructural with that of $W(CO)_3(PCy_3)_2$[2a] with the important differences that all the hydrogens were located for the Cr complex and that the shorter Cr-P and Cr-C bond lengths increase steric crowding around the metal center. A comparison of relevant structural differences between the Cr and W complexes is given in Table IX. The Cr-H agostic distance of 2.240 Å is slightly shorter than that calculated for the W analogue (Table IX) and is one of the few determined crystallographically.[12a,13]

The increased importance of steric factors in the solution thermochemistry of the chromium complex is shown by the data

(12) (a) Crabtree, R. H.; Hamilton, D. G. *Adv. Organomet. Chem.* **1988**, *28*, 299 and references therein. (b) Brown, C. F.; Ishikawa, Y.; Hackett, P. A.; Rayner, D. M. *J. Am. Chem. Soc.* **1990**, *112*, 2530. (c) Morse, J. M., Jr.; Parker, G. H.; Burkey, T. J. *Organometallics* **1989**, *8*, 2471.

(13) Brookhart, M.; Green, M. L. H.; Wong, L. L. *Prog. Inorg. Chem.* **1988**, *36*, 1.

for heats of ligand binding in Table II. The presence of an agostic bond in each of these complexes complicates discussion of bond strengths in these systems. Infrared and structural studies show that all three metals have the sixth site occupied by a three-center M···H-C bond.[2] For an agostic β-alkyl group,[13] calorimetric studies of ligand addition measure the M-L bond strength relative to the weak agostic bond strength. For this reason, we can compare only relative bond strengths in these complexes. Determination of "absolute" bond strengths requires knowledge of the agostic bond strength, which could be different for each metal. Literature estimates indicate this is in the range of 10–15 kcal/mol.[12a] Gas-phase data for binding of alkanes to $W(CO)_5$ have recently been determined to be in the range 7–11 kcal/mol.[12b] Photoacoustic work by Morse, Parker, and Burkey has shown that bond strengths in $M(CO)_5$(heptane) bonds are 10, 9, and 13 kcal/mol for Cr, Mo, and W, respectively,[12c] and that bonds to cyclohexane are 2–3 kcal/mol stronger than bonds to heptane. Since the agostic bond is on a trajectory toward oxidative addition,[12a] increased electron density on the metal in the phosphine-substituted complexes $M(CO)_3(PR_3)_2$(alkane) might be expected to lead to stronger agostic bonds. The addition of CO to the complex $W(CO)_3(PCy_3)_2$ in solution[4] is 16 kcal/mol less exothermic than the addition to $W(CO)_5$ in the gas phase.[14] This serves as a first approximation for the agostic bond in the tungsten complex and is in rough agreement with the alkane-binding studies discussed above.

Relative heats of binding for all three metals show the order of ligand preference to be $P(OMe)_3 > py > N_2 > H_2$. The data for Mo and W are nearly parallel. Heats of binding of all ligands to Mo are 3 ± 1 kcal/mol less than those for W. That is not the case for chromium. Only for the relatively bulky ligands py and $P(OMe)_3$ is the enthalpy of binding to Cr less exothermic than the corresponding value for Mo.

Gas-phase studies[14] have shown that the M–CO bond strengths in $M(CO)_6$ are as follows (kcal/mol): Cr, 36.8; Mo, 40.5; W, 46.0. The consistently higher heats of binding to W are in keeping with this order. For N_2 and H_2, the heats of binding to Cr and Mo are, for all practical purposes, identical. Since these values are relative to the agostic bond, it seems possible that the chromium complex has a weaker agostic bond, which could make its ligand addition reactions somewhat more exothermic than expected. The bond angles in the five-membered Cr-P-C-C-H[11a] ring, however, are identical to those in the W analogue and appear to show no additional strain.

Enthalpies of ligand addition of the bulkier ligands py and $P(OMe)_3$ show clear preference for Mo over Cr on the order of 6–7 kcal/mol. This can probably be ascribed to increased steric crowding for the first-row metal. This is best viewed by calculating the enthalpy of the ligand-exchange reaction (17). Using data

$$Cr(CO)_3(PCy_3)_2(N_2) + Mo(CO)_3(PCy_3)_2(py) \rightarrow Cr(CO)_3(PCy_3)_2(py) + Mo(CO)_3(PCy_3)_2(N_2) \quad (17)$$

from Table II, the enthalpy of this reaction is calculated to be +6 kcal/mol. This value does not involve knowledge of the agostic bond strengths, and we view it as direct measurement of steric strain in the first-row complex. Electronic factors can never be ruled out; however, all of the ligands involved are relatively "soft", and increased "steric pressure" seems to be the best explanation. Of the 18 possible ligand-exchange reactions between metals that can be calculated from Table II, only those removing pyridine or trimethyl phosphite from chromium and replacing it with a smaller ligand are significantly exothermic. Additional ligand-binding studies and molecular mechanics calculations are planned for this system.

The facile displacement of tricyclohexylphosphine by pyridine as shown in eq 7 also indicates the increased role of steric factors for the first-row metal. Such reactions do not appear to occur for molybdenum and tungsten. In strain-free environments, the $M-PR_3$ bond is almost always stronger than the M–py bond for low-valent metals. On the basis of the discussions above and the calorimetric data for other ligands,[15] it seems likely that *bulky* ligands binding to the chromium complex are destabilized an additional 3–7 kcal/mol relative to those binding to molybdenum and tungsten due to steric factors alone in these complexes.

The rates of dissociation of the M–py bond parallel the thermodynamic bond strengths. The rate of ligand dissociation is in the order Cr > Mo > W (4800/300/1). This follows the order of the M–L bond enthalpies. It is in contrast to simple substitution reactions where molybdenum is often observed to be the most labile. The chromium–pyridine bond is so weak that it has a half-life for dissociation on the millisecond time scale at room temperature.

In spite of the steric crowding at the metal center, these reactions are probably associative in character. Enthalpies of activation for ligand dissociation are all about 4 kcal/mol higher than enthalpies of ligand binding. Since, as discussed above, the agostic bond strength is probably on the order of 10–15 kcal/mol in these complexes, dissociation would be expected to be partially associative in character on the basis of energetic considerations. Kinetic isotope-effect studies reported[8] earlier for the tungsten complex also support an internal associative displacement as shown in eq 18. The entropies of activation for dissociation of pyridine

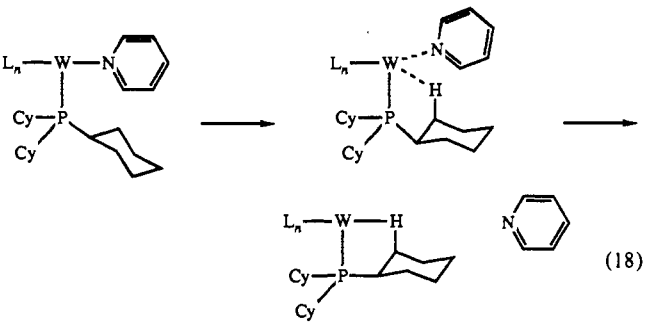

(18)

also imply a fair amount of ordering in the transition state. The thermodynamic data for the dissociation of pyridine indicate that ΔS = 28.8 ± 5.7 cal/(mol deg), a value in reasonable agreement with statistical mechanical estimates.[9] The entropies of activation for the k_1 step are all positive but less than the value for full dissociation. Due to thermal instability, these complexes were only studied over a limited temperature range (5–35 °C), and so conclusions regarding entropy of activation data are tentative. In spite of this, the entropy of dissociation for the chromium complex is smallest and may imply that the transition state in this system is more highly ordered due to steric factors. Additional work to measure volumes of activation in these systems is planned.[16]

In contrast to its faster rate of ligand dissociation, the chromium complex shows significantly slower rates of ligand addition. Thus $Cr(CO)_3(PCy_3)_2$ reacts nearly 2 orders of magnitude slower with $P(OMe)_3$ than does the analogous molybdenum complex. The degree of ligand discrimination is also higher for chromium. The rate of reaction with pyridine is 37 times faster than with phosphite for chromium, compared to a value of 17 for molybdenum. Enhanced ligand selectivity for the chromium complex is in keeping with its smaller size. In terms of kinetic selectivity, the molybdenum complex is remarkably similar to the tungsten complex. Thus the relative rates of reaction of py/$(POMe)_3$/PPh_2Me are 51/17/1 for Mo and 51/16/1 for W. This is probably due to the fact that incoming ligands "see" a very similar picture as they approach the molybdenum and tungsten complexes.

The combination of faster rates of ligand dissociation and slower rates of ligand association results in the chromium complex not obeying simple steady-state theory. The steady increase in M–L bond strengths results in a deepening of the reaction profile shown in Figure 6 in going from Cr to Mo to W.

(14) Smith, G. P. *Polyhedron* **1988**, *7*, 1605.

(15) This conclusion is based on calorimetric data on ligand substitution for a number of low-valent group VI complexes: (a) Nolan, S. P.; de la Vega, R. L.; Hoff, C. D. *Organometallics* **1986**, *5*, 2529. (b) Mukerjee, S. L.; Nolan, S. P.; Hoff, C. D.; de la Vega, R. L. *Inorg. Chem.* **1988**, *27*, 81. (c) Mukerjee, S. L.; Gonzalez, A. A.; Zhang, K.; Hoff, C. D. Unpublished results.

(16) Lewis, N. A.; Taveras, D.; Hoff, C. D. Work in progress.

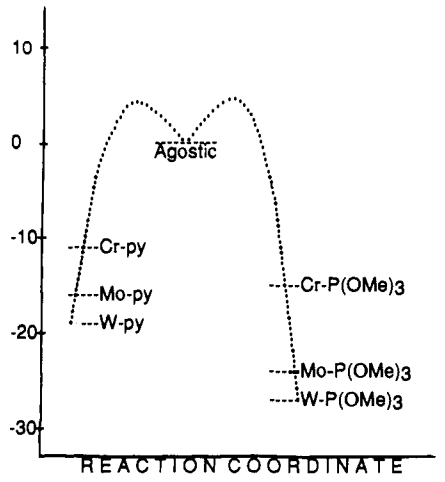

Figure 6. Potential energy diagram (enthalpy of reaction in kcal/mol) for reactions of $M(CO)_3(PCy_3)_2(py)$ with $P(OMe)_3$ (M = Cr, Mo, W). Enthalpies of activation are shown for W only, but values for Cr and Mo are similar, as shown in Table VIII.

Conclusion

It is well-known that the M-L bond lengths for low-valent complexes are in the order Cr < W = Mo and indeed were found to be 0.10–0.14 Å shorter in $Cr(CO)_3(PCy_3)_2$ compared to its W analogue. The consequences of pulling the ligands in along the metal axis will be to increase the effective "cone angle",[17] as illustrated in Figure 5. As a result, the steric environment facing an incoming ligand is more severe for the first-row metal. This is seen in faster rates of dissociation, slower rates of association, and lower than expected enthalpies of ligand binding for bulky ligands. In addition, larger ligand selectivities and different types of reactivity are also shown; however, these effects cannot be attributed to stark or sudden changes. It seems most likely that the chromium complex suffers an additional destabilization due to its smaller size and that this is on the order of 3-7 kcal/mol for bulky ligands. The experimental data reported here provide some of the first direct comparisons of these effects for a complete series of sterically crowded complexes. Additional thermodynamic and kinetic studies on these and related complexes are in progress.

Acknowledgment. Support of this work by National Science Foundation Grant CHE-8618753 is gratefully acknowledged. Special thanks are due to Dr. Nita Lewis and Mr. Daniel Taveras at the University of Miami for use of the stopped-flow equipment.

Supplementary Material Available: Tables giving additional data for the crystal structure of $Cr(CO)_3(P(C_6H_{11})_3)_2$, including atomic coordinates and equivalent isotopic displacement coefficients, bond lengths, bond angles, anisotropic displacement coefficients, and H atom coordinates and isotropic displacement coefficients (10 pages); tables of observed and calculated structure factors (21 pages). Ordering information is given on any current masthead page.

(17) Tolman, C. A. *Chem. Rev.* **1977**, *77*, 313.

The Role of the 16-Electron $[(\eta^5\text{-}C_5Me_5)Ru(NO)]$ Transient in the Formation of Dinuclear Complexes and in Oxidative Addition Reactions

John L. Hubbard,*[1a] Andre Morneau,[1b] Robert M. Burns,[1a] and Christopher R. Zoch[1a]

Contribution from the Department of Chemistry and Biochemistry, Utah State University, Logan, Utah 84322-0300, and Department of Chemistry, The University of Vermont, Burlington, Vermont 05405. *Received May 1, 1991*

Abstract: The formation of $[Cp^*Ru(\mu\text{-}NO)]_2$ (**2**) from the treatment of $Cp^*Ru(NO)Cl_2$ (**1**) with Zn dust in EtOH is preceded by the formation of an intermediate complex $[Cp^*Ru(\mu\text{-}NO)Cl]_2$ (**4**) containing a formal Ru-Ru single bond ($Cp^* = \eta^5\text{-}C_5Me_5$). Complex **4** is fully characterized, including a single-crystal X-ray structure: monoclinic space group $P2_1/n$, a = 8.272 (3) Å, b = 14.722 (5) Å, c = 9.863 (3) Å, β = 107.42 (2)°, Z = 4, R_w = 5.28%, based on 1301 observed data ($F > 4.0\sigma(F)$). The structure shows a centrosymmetric trans geometry with bridging nitrosyl ligands, terminal chloride ligands, and a Ru-Ru distance of 2.684 (2) Å. Purified complex **4** reacts further with Zn dust in EtOH to give **2** quantitatively. Complex **4** is formed together with $Cp^*Ru(NO)(CH_2Cl)Cl$ (**6**) in the reaction of $Cp^*Ru(NO)Ph_2$ (**5a**) with CH_2Cl_2. The fact that complex **4** is formed in high yield from the thermolysis of an equimolar mixture of **5a** and **1** in ethanol suggests that any $[Cp^*Ru(NO)]$ transients produced in the Zn reaction are efficiently trapped to complex **4** by excess **1**. Crossover experiments involving **5a** and $Cp^*Ru(NO)(p\text{-tolyl})_2$ (**5b**) help verify that the generation of the 16-electron $[Cp^*Ru(NO)]$ species is the first process to occur when $Cp^*Ru(NO)(aryl)_2$ complexes are thermalized in chlorinated and non-chlorinated solvents. Thermolysis of **5a** in 1,2-dichloroethane gives complex **4** and ethylene, apparently through the generation of an unstable β-chloroethyl complex which decomposes to ethylene and dichloride complex **1**; the absence of **1** in the final reaction residue is attributed to its consumption by $[Cp^*Ru(NO)]$ transients, leading to **4** as the only observed organometallic product.

Introduction

Although certain 16-electron $(\eta^5\text{-}C_5R_5)ML$ species are known to activate C-H and C-halogen bonds,[2] their role in the formation and reactivity of the 32-electron $[(\eta^5\text{-}C_5R_5)M(\mu\text{-}L)]_2$ dimers (containing formal metal-metal double bonds) is less clear (R = H, CH_3; M = Rh, Ir; L = CO, PR_3, CNR).[3] Jones and Feher have reported the formation of $[Cp^*Rh(\mu\text{-}CNR)]_2$ complexes from the reduction of $Cp^*Rh(CNR)X_2$ precursors,[4] but have recently called into question the presence of a $[Cp^*Rh(CNR)]$ 16-electron transient, since no C-H activation is observed ($Cp^* = \eta^5\text{-}C_5Me_5$).[5]

(1) (a) Utah State University. (b) University of Vermont.
(2) (a) Bergman, R. G. *J. Organomet. Chem.* **1990**, *400*, 273-282 and references therein. (b) Graham, W. A. G. *J. Organomet. Chem.* **1986**, *300*, 81 and references therein. (c) Werner, H. *Angew. Chem., Int. Ed. Engl.* **1983**, *22*, 927-949.
(3) (a) Seidler, M. D.; Bergman, R. G. *Organometallics* **1983**, *2*, 1897-1899. (b) Seidler, M. D. Ph.D. Thesis, University of California, Berkeley, CA, 1984.
(4) Jones, W. D.; Feher, F. J. *Organometallics* **1983**, *2*, 686-687.
(5) Jones, W. D.; Duttweiler, R. P.; Feher, F. J. *Inorg. Chem.* **1990**, *29*, 1505-1511.

0002-7863/91/1513-9176$02.50/0